https://doi.org/10.5194/hess-2019-335
Preprint. Discussion started: 8 July 2019

Hydrology and Earth System Sciences
Discussions

Simulations of future changes in thermal structure of Lake Erken: Proof of concept for ISIMIP2b lake sector local simulation strategy

Ana I. Ayala[1, 2], Simone Moras[1], Don C. Pierson[1]

[1]Department of Ecology and Genetics, Limnology, Uppsala University, Uppsala, 752 36, Sweden
[2]Department of Applied Physics, Nonlinearity and Climate Group, University of Geneva, Geneva, CH-1211, Switzerland

Correspondence to: Ana I. Ayala (isabel.ayala.zamora@ebc.uu.se)

Abstract. This paper, as a part of Inter-Sectoral Impact Model Intercomparison Project (ISIMIP2b), assesses the impacts of different levels of global warming on the thermal structure of Lake Erken (Sweden). The GOTM one-dimensional hydrodynamic model was used to simulate water temperature when using ISIMIP2b bias-corrected climate model projections as input. These projections have a daily time step, while lake model simulations are often forced at hourly or shorter time steps. Therefore, it was necessary to first test the ability of GOTM to simulate Lake Erken water temperature using daily vs hourly meteorological forcing data. In order to do this three data sets were used to force the model: 1) hourly measured data; 2) daily average data derived from the first data set and; 3) synthetic hourly data created from the daily data set using Generalized Regression Artificial Neural Network methods. This last data set is developed using a method that could also be applied to the daily time step ISIMIP scenarios to obtain hourly model input if needed. The lake model was shown to accurately simulate Lake Erken water temperature when forced with either daily or synthetic hourly data. Long-term simulations forced with daily or synthetic hourly meteorological data suggest that by 2099 the lake will undergo clear changes in thermal structure, for RCP 2.6 surface water temperature was projected to increase from 0.87 to 1.48 ºC and from 0.69 to 1.20 ºC when the lake model was forced at daily and hourly resolutions respectively, and for RCP 6.0 these increases were projected to range from 1.58 to 3.58 ºC and from 1.19 to 2.65 ºC when the lake model was also forced at daily and hourly resolutions. Changes in lake stability were projected to increase significantly and the stratification duration was projected to be longer by 9 to 16 days and from 7 to 13 days under RCP 2.6 scenario and from 20 to 33 days and from 17 to 27 under RCP 6.0 scenario for daily and hourly resolutions. Model trends were very similar when using either the daily or synthetic hourly forcing, suggesting that the original climate model projections at a daily time step can be sufficient for the purpose of simulating water temperature in the lake sector in ISIMIP.

1 Introduction

The thermal structure of lakes is controlled by heat and energy exchange across the air-water interface, which is in turn determined by meteorological forcing (Woolway et al., 2017). Climate change will affect air-water energy exchanges and alter the temperature regime and mixing of lakes (Mesman et al., 2019 submitted). For example, increases in air temperature

https://doi.org/10.5194/hess-2019-335
Preprint. Discussion started: 8 July 2019


Hydrology and Earth System Sciences
Discussions

results in a consequent warming of lake water temperature (Sahoo et al. 2015) causing shorter ice-cover periods (Kainz et al., 2017; Butcher et al. 2015), longer stratified period (Ficker et al., 2017; Woolway et al., 2017; Magee and Wu, 2017) and increased lake stability (Rempfer et al., 2010; Hadley et al., 2014). Decreasing wind speed can induce more stable and long-lasting stratification (Woolway et al. 2017) and increased epilimnetic temperature (Stefan et al., 1996).

The most direct effect of climate change on lakes is a warming of the lake surface temperature. For example, global average warming rates of 0.34°C decade^{-1} have been observed between 1985 and 2009 by O'Reilly et al. (2015). Hypolimnetic temperature responds less clearly to warming and has been observed to be warming, cooling or not changing significantly with increasing air temperature (Shimoda et al., 2011; Butcher et al., 2015; Winslow et al. 2017). And, these changing water temperatures have also led to an increased stability and duration of stratification (Butcher et al., 2015; Kraemer et al., 2015).

A final consequence of warming lake temperature is projected to be the shift in the mixing regime (Krillin, 2010; Shimoda et al., 2011; Shatwell et al., 2019; Woolway and Merchant, 2019). For example, loss of ice cover in deep lakes is likely to turn amictic lakes into cold monomictic lakes, and cold monomictic lakes into dimictic lakes (Nõges et al., 2009).

These changes in lake water temperature and thermal stratification influence lake ecosystem dynamics (MacKay et al., 2009). Increases in stratification stability and duration can intensify hypolimnetic oxygen depletion (Foley et al., 2012; Schwefel et al., 2016) and hence induce enhanced internal phosphorous loading (North et al., 2014), increase the release of dissolved iron and manganese from sediments (Schultze et al., 2017) and also increase methane emissions (Grasset et al., 2018). Warming lake temperature affects biological rates of metabolism, growth and reproduction (Rall et al., 2012) and can promote cyanobacterial blooms (Paerl and Paul, 2012). When coupled to a reduction in oxygen-rich water, warming water temperature leads to a lower fish populations (O'Reilly et al., 2003; Yankova et al., 2017).

Numerical modeling plays a key role in estimating the sensitivity of the lakes to changes in the climate. One-dimensional lake models are widely used due to their computational efficiency and the realistic temperature profiles they produce. Several studies have investigated the impacts of climate change on lake water temperature under Regional Climatic Model (RCM)/Global Climatic Model (GCM) projections (Persson et al., 2005; Kirillin, 2010; Perroud and Goyette, 2010; Samal et al., 2012; Ladwig et al., 2018; Shatwell et al., 2019; Woolway and Merchant, 2019). Commonly when undertaking climate change impact studies, hydrodynamic lake models are driven by daily resolution RCM/GCM outputs. Bruce et al. (2018) undertook a comparative analysis of model performance using daily and hourly resolution meteorological forcing data, and found a better agreement between observations and predictions of full-profile temperature when the lakes were modelled using hourly meteorological input. This reinforces the importance of diurnal forcing on 1-D model predictive capability.

The purpose of this study is therefore (1) to test the ability of a one dimensional-hydrodynamic model (GOTM) to simulate the water temperature of Lake Erken (Sweden) using daily vs hourly meteorological forcing data for the period 2006-2016, (2) develop a reliable method to disaggregate daily meteorological data to a hourly synthetic product that can be used to force the GOTM model and (3) convert daily GCM outputs available from the ISIMIP project into hourly meteorological variables and assess the impacts on the thermal structure of Lake Erken at different levels of global warming when GOTM is

https://doi.org/10.5194/hess-2019-335
Preprint. Discussion started: 8 July 2019


Hydrology and Earth System Sciences
Discussions

driven by hourly and daily model projections. In fulfilling these objectives this study provides the first evaluation of modelling methods that will be used by the lake sector within the ISIMIP.

2 Material and Methods

2.1 Study site

Lake Erken (59°51'N, 18°36'E) is a mesotrophic lake located in east central Sweden, with a maximum depth of 21 m, a mean depth of 9 m and a surface area of 23.7 km^2. The lake is dimictive with summer stratification usually occurring beginning in May-June and ending in August-September, while ice cover occurs from December-February to April-May (Persson and Jones, 2008). It is the lake's relatively shallow depth and large surface area, which leads to large inter-annual variability in the timing and patterns of thermal stratification. The lake has a retention time of approximately 7 years and shows annual variations in water level that are less the 1 m (Pierson et al., 1992; Moras et al., 2019 in review).

2.2 Lake model

General Ocean Turbulence Model (GOTM) is a one dimensional water column model that simulates the most important hydrodynamic and thermodynamics processes related to vertical mixing in natural waters (Umlauf et al. 2005). GOTM was developed by Burchard et al. (1999) for modelling turbulence in the oceans, but it has been recently adapted for use in hydrodynamic modelling of lakes (Sachse et al., 2014). The strength of GOTM is the vast number of well-tested turbulence models that have been implemented spanning from simple prescribed expressions for the turbulent diffusivities up to complex Reynolds-stress models with several differential transport equations. Typically GOTM is used as a stand-alone model for investigating the dynamics of boundary layers in natural waters but it can also be coupled to a biogeochemical model using the Framework for Aquatic Biogeochemical Models (FABM) (Bruggeman and Bolding, 2014).

2.3 Data sets

Meteorological data required to drive GOTM were wind speed (m s^{-1}), atmospheric pressure (hPa), air temperature (ºC), relative humidity (%), cloud cover (dimensionless, 0-1), short-wave radiation (W m^{-2}) and precipitation (mm day^{-1}). Local meteorological variables were collected either from a small island 500 m offshore from the Erken Laboratory, or the Swedish Meteorological Hydrological Institute (SMHI) Svanberga Station just behind the laboratory. The Malma Island meteorological Station (59.83909º N, 18.629558º E) measured air temperature at 2 m above water surface, wind speed at 10 m above the water surface and short-wave radiation. These data were measured at one minute intervals and saved as 60 min mean values. Mean sea level pressure relative humidity and precipitation were measured at the Svanberga Meteorological Station at 800 m from the Malma Island Meteorological Station (59.8321º N, 18.6348º E) with a frequency of 60 minutes. Hourly cloud cover was recorder from Svenska Högarna Station (59.4445 N, 19.5059 E) at 69 km south-east of Lake Erken.

https://doi.org/10.5194/hess-2019-335
Preprint. Discussion started: 8 July 2019


Hydrology and Earth System Sciences
Discussions

The measured hourly meteorological data were used to construct two other data sets that would replicate the data resolution that could potentially be used to force the GOTM model with ISIMIP scenarios. First to test running the model at a daily resolution a daily data set was created by averaging the hourly one (except for precipitation which was summed). Secondly, this mean daily data set was disaggregated to form a synthetic hourly data set. Hourly estimations of air temperature wind speed, relative humidity and short wave radiation were estimated using the GRNN methods described below. For atmospheric pressure and cloud cover, mean daily values were assumed to be constant over the day. Precipitation was disaggregated assuming a uniform distribution of the daily total (Waichler and Wigmosta, 2003).

Since both of these data sets are based on the same measured hourly data, comparison of model simulations of lake water temperature, allow the importance of hourly vs daily temporal resolution in the forcing data to be evaluated, and also the improvements in model performance that can be obtained from daily data (as in the ISIMIP scenarios) when imposing a diurnal cycle on the mean daily data.

Water temperature data needed to calibrate the model was monitored from an automated floating station (59.84297º N, 18.635433º E). During ice-free conditions measurements were made every 0.5 m from 0.5m to a depth of 15 m. Measurements were made every minute, and a mean of these measurements was stored every 30 minutes.

2.4 Climate scenarios

The ISIMIP climate scenarios are bias-corrected global climate model (GCM) (Hempel et al., 2013) data made available at daily temporal and 0.5º horizontal resolution for the variables listed in Table 1. Data from the grid box overlying Lake Erken were available from the GFDL-ESM2M, HadGEM2-ES, IPSL-CM5A-LR and MIROC5 GCM models that were each run under four emission scenarios. These included a scenario having historical levels of atmospheric CO_2 between 1861 and 2005, and two future scenarios (RCP 2.6 and RCP 6.0) from 2006 to 2099. RCP 2.6 is the strongest mitigation pathway that is expected to limit mean global warming to between 1.5 and 2 ºC. RCP 6.0 is a low mitigation pathway where global warming is projected to rise to between 2.5 and 4 ºC by the end of century compared to the pre-industrial period (Frieler et al., 2017).

2.5 Temporal disaggregation of meteorological forcing data

The GCM scenarios have a daily time step, while lake model simulations are often forced with meteorological data at hourly or shorter time steps. Therefore, it was necessary to test the ability of the GOTM model to simulate Lake Erken water temperature using daily vs hourly meteorological forcing data, and to evaluate the need to disaggregate the daily GCM scenarios to a shorter time step.

Kathib and Elmernreich (2015) proposed a generalized regression artificial neural network (GRNN) model for predicting hourly variations in short-wave radiation from daily average measurements. Using the GRNN model to predict hourly solar radiation required ten geographical and climatic variables as input including hour, day, month, latitude, longitude, daily

https://doi.org/10.5194/hess-2019-335
Preprint. Discussion started: 8 July 2019


Hydrology and Earth System Sciences
Discussions

average short-wave radiation, daily precipitation, the solar elevation associated with the hour, and time of sunrise and sunset. Precipitation was used to define wet and dry status that affected atmospheric attenuation (Waichler and Wigmosta, 2003).

There are also empirical models developed for calculating hourly air temperature, wind speed and relative humidity. Parton and Logan (1981) proposed a model for predicting diurnal variations in air temperature. Daylight air temperature was modelled using a sine wave with the minimum value at sunrise, maximum value at solar noon and mean value at sunset. Night-time air temperature was modelled as a linear interpolation between air temperature of the previous day and sunrise air temperature of the following day. Guo et al. (2013) generated hourly values of wind speed by computing a cosine function dependent on the mean daily wind speed, the maximum daily wind speed and the hour of the day when the wind speed is maximum. Waichler and Wigmosta (2003) estimated hourly values relative humidity from daily maximum and minimum air temperature and daily maximum and minimum relative humidity. Using these studies as guidance, we developed GRNN models to predict hourly a) air temperature, b) wind speed and c) relative humidity. The input parameters for each GRNN model were: a) hour, day, month, latitude, longitude, mean daily air temperature, daily maximum and minimum air temperature, daily precipitation, hourly solar angle, and time of sunrise and sunset for predicting hourly air temperature; b) hour, day, month, latitude, longitude and daily wind speed for predicting wind speed; and c) hour, day, month, latitude, longitude, mean daily relative humidity, daily precipitation, hourly air temperature and hourly short-wave radiation for predicting relative humidity. More detailed description of the GRNN methods and models are given in the supplementary material to this paper.

2.6 Model calibration and validation

Calibration of the GOTM model was conducted to adjust the model parameters within their feasible range in order to minimize the error between measured and modelled temperature (Huang and Liu, 2010). A period of 8 years was selected for the calibration of GOTM, 2006-2014 (included 1 year spin-up followed by 7 years for calibration). The model parameters that were calibrated were surface heat-flux factor (shf_factor), short-wave radiation factor (swr_factor), wind factor (wind_factor), minimum turbulent kinetic energy (k_min) and e-folding depth for visible fraction of light (g2). The program used to calibrate the model was ACPy (Auto-Calibration Python), developed by Bolding and Bruggeman (https://bolding-bruggeman.com/portfolio/acpy/), it uses a differential evolution algorithm which calculates a log likelihood function based on comparing the modelled and measured water temperature (Storn and Price, 1997). The validation period was 2 years 2015-2016.

For both calibration and validation, daily average water temperatures were simulated when GOTM was forced using the three meteorological data sets described above: measured average daily, measured average hourly and synthetic hourly data. Model simulated profiles of mean daily water temperature were then compared to mean daily measured water temperature. During calibration the model was run approximately 10000 times to obtain a stable solution specifying the optimal parameter set, for each meteorological forcing data set. The details of the feasible range of model parameters and calibrated parameters are given in Table 2. The same calibrated parameters were used to predict the thermal structure under GCM scenarios.

https://doi.org/10.5194/hess-2019-335
Preprint. Discussion started: 8 July 2019


Hydrology and Earth System Sciences
Discussions

Model performance was evaluated by comparing average daily modelled and measured temperature profiles and other metrics describing the lake thermal structure (surface and bottom temperature, volumetrically weighted averaged whole lake temperature, Schmidt stability and thermocline depth). The model efficiency coefficients used were mean bias error (MBE), root mean squared error (RMSE) and Nash-Sutcliffe efficiency (NSE) (Nash and Sutcliffe, 1970).

2.7 Thermal indices

A range of thermal metrics: surface temperature, bottom temperature and thermocline depth were derived on a daily bases from the daily simulated lake temperature profiles. Also from these profiles, Schmidt stability and volumetric weighted mean whole lake temperature were estimated using Lake Analyzer (Read et al., 2011). The duration of thermal stratification was calculated as the longest continuous period when the water column density difference from the bottom to surface of the lake was greater than 0.1 kg m^{-3} (according to ISIMIP2b lake sector protocol). The date of the onset and loss of the thermal stratification was defined as the first time that this density difference persisted for more than 5 days or was absent for at least 5 days (Kraemer et al., 2015).

3 Results

3.1. Hourly meteorological modelling

Air temperature, short-wave radiation, relative humidity and wind speed were temporarily disaggregated into hourly values from mean daily data, using the GRNN models. A database was constructed using 8 years of measurements. From this whole set of data, the first 5-years of data, that is, from 2008 to 2012, were used for training, and 3-years of data from 2013 to 2015 were used for validating the results obtained. The accuracy of the trained network was assessed by comparing the predicted output with actual measured hourly data. The results are presented in Supplementary Fig. 1,2,3,4. The performance index for training and validating sets of GRNN models are given in terms of MBE, RMSE and NSE (see Table 3).

There was a close agreement between GRNN model predictions and measured meteorological data as shown in Fig. 1 for a single year data. For air temperature we obtained a NSE of 0.999 and 0.940 and RMSEs of 0.256 and 0.318 ºC for the training and validate data sets. The MBE values indicated a slightly cold temperature bias (MBE of -1.70 10^{-4} and -0.057 ºC). Short-wave radiation and relative humidity predictions for the training data set also show an accurate model performance with a NSE of 0.999 and 0.998 (RMSEs of 6.345 W m^{-2} and 0.790 %) respectively. For the validation data set the GRNN models performed somewhat worse, NSE of 0.870 and 0.686 (RMSE of 8.196 W m^{-2} and 1.021 %) for the short-wave radiation and relative humidity predictions. Wind speed was the variable showing the poorest performance with a NSE of 0.779 and 0.584 (RMSE of 1.060 and 1.370 m s^{-1}) for the training and validate data sets. In general, the calculated MBE values in supplementary Fig. 5 show that the GRNN model tended to overestimate wind speed (MBE of 0.63±0.92 m s^{-1}) when the observed wind speed is lower than or equal to 3.84 m s^{-1}, whereas projected wind speed tends to be underestimated (MBE of -0.78±1.17 m s^{-1}) when the observations are greater than 3.84 m s^{-1}.

https://doi.org/10.5194/hess-2019-335
Preprint. Discussion started: 8 July 2019


Hydrology and Earth System Sciences
Discussions

3.2. Lake model performance

Temperature observations and simulations, for the three configurations of meteorological forcing data for both calibration and validation periods, are shown in Fig. 2. Model performance metrics associated with these simulations are provided in Fig. 3 and Table 4.

These data demonstrate that GOTM was able to accurately reproduce the measured temperature profiles. For an average of all three calibration data sets a RMSE of 0.81 ºC and NSE of 0.96 was obtained. Temperature simulations for the validation period were more accurate (average RMSE of 0.66 ºC and NSE of 0.97) than for the calibration period (average RMSE of 0.95 ºC and NSE of 0.94), but in both periods the model performance was considered acceptable. When comparing the metrics of model fit associated with simulations forced with the three different input data sets the RMSEs for calibration period ranged from 0.88 to 1.04 ºC, with lower error levels associated with simulations driven by hourly meteorological data sets, whereas for the validation period the RMSEs were comparable for all data sets, with slightly lower RMSE 0.63 ºC for the temperature simulations driven by daily meteorological data. The MBE values indicated a slight cold temperature bias (average MBE of -0.05 ºC).

The model performance predicting just surface temperatures (average RMSE of 0.63 ºC and NSE of 0.98) was better that estimations of the full temperature profiles. The MBE, showed that GOTM tended to produce a cold temperature bias (average MBE of -0.10 ºC). As would be expected the simulations of bottom temperature were slightly less accurate having average RMSE of 0.96 ºC and NSE of 0.90, with lower RMSE values for the validation period (average RMSE of 0.67 ºC) than the calibration period (average RMSE of 1.25 ºC), but in contrast to the surface temperature, there was a slight warm temperature bias (average MBE of 0.06 ºC). The best fits in the bottom temperature simulations were those driven by the measured hourly meteorological data set during the validation period (RMSE of 0.59 ºC and NSE of 0.97) and the synthetic hourly meteorological data, during the calibration period (RMSE of 1.16 ºC and NSE of 0.87). When evaluating the simulations of volumetrically weighted averaged whole lake temperatures we found that model errors were of a similar magnitude with an average RMSE of 0.53 ºC and NSE of 0.98, tending to a slight cold temperature bias (average MBE of -0.08 ºC).

The calculation of Schmidt stability, the resistance to mechanical mixing due to the potential energy inherent in the density stratification of the water column (Read et al., 2011), was also well simulated for using all three data sets (average RMSE of 17.24 J $m^{-2}$and NSE of 0.88). The lowest RMSE values were for the validation period (average RMSE of 13.34 J m^{-2}) whereas during the calibration period values were slightly greater (average RMSE of 21.14 J m^{-2}). Thermocline depth, defined as the depth of the maximum density gradient, was the parameter with the poorest performance (average RMSE of 3 m). The MBE values (average MBE of 0.80 m) indicate a bias towards under prediction of thermocline depth (shallower thermocline depths).

https://doi.org/10.5194/hess-2019-335
Preprint. Discussion started: 8 July 2019


Hydrology and Earth System Sciences
Discussions

3.3. Long-term modelled changes in thermal stratification

The lake model was forced by four climate model projections and three emissions scenarios (historical, RCP 2.6 and RCP 6.0) available from ISIMIP for GFDL-ESM2M, HadGEM2-ES, IPSL-CM5A-LR and MIROC5 using their original daily resolution and also at hourly resolution using meteorological disaggregated data developed using the GRNN models describe above. Simulated water temperatures for the historical, RCP 2.6 and RCP 6.0 scenarios under daily IPSL-CM5A-LR projections are presented as temperature isopleths in Fig. 4. These were created by averaging the daily temperature profiles for all years associated with each of the emission scenarios. These mean scenario temperature isopleths provide a clear visualization of how for future scenarios surface and bottom water temperatures are projected to increase with stronger and deeper stratification, an earlier stratification onset and later fall overturn and consequently longer stratification period.

Anomalies were calculated to further evaluate these impacts on lake water temperature and thermal stratification. The anomalies were computed for each GCM by taking the difference between the annual average of each year (2006-2099) from RCP 2.6 and 6.0 scenarios and the average for the entire period 1975-2005 from the historical scenario. From these average yearly values were calculated using the months between April and September, due to the fact that the GOTM model was not able to simulate lake ice and winter water temperatures at the same level of accuracy as during the remainder of the year. The slope of the significant trends were evaluated by least-squares linear regression, except when the residuals did not follow a normal distribution. Then the non-parametric Mann-Kendall test for the significance of trends and the Theil-Sen method (Theil, 1950; Sen, 1968) to estimate the slope of the significant trends were used instead.

In general there were significant changes in all the metrics describing thermal stratification evaluated in this study as can be seen from the frequency distribution of yearly anomalies in Fig. 5,6 and the detailed statistics presented in Table 5. The exception to this is the GFDL-ESM2M model which showed lower or non-significant changes. The other three models showed more consistent and larger anomalies as compared to GFDL-ESM2M. Similar trend in the anomaly distributions were seen when the GOTM model was forced with either mean daily or synthetic hourly data. Detailed comparison of the results derived using the two different forcings (Table 5) suggest that the simulated changes are slightly greater when simulations are forced with the mean daily data. However, in both cases the same direction in the trends and the same overall descriptions of change is found.

Rates of change in whole-lake temperature calculated for over the length for RCP2.6 and 6.0 scenarios were projected to increase except in the case of GFDL-ESM2M which showed weaker or non-significant changes for all measures of thermal stratification. Simulated changes were generally slight less for the simulations driven by daily forcing data as shown by the figures in parentheses For RCP 2.6 rate of change ranged from 0.06 to 0.10 ºC decade^{-1} (0.05 to 0.08 ºC decade^{-1}), the values in bracket refer to future projections when the lake model was forced at hourly resolutions. For RCP 6.0, the projected rate of change ranged from 0.15 to 0.27 ºC decade^{-1} (0.11 to 0.19 ºC decade^{-1}). IPSL-CM5A-LR projected the largest increase being 0.59 ºC (0.43 ºC) under RCP 2.6 ºC and 2.51 ºC (1.79 ºC) under RCP 6.0.

https://doi.org/10.5194/hess-2019-335
Preprint. Discussion started: 8 July 2019

Hydrology and Earth System Sciences
Discussions

Surface temperature is warmed significantly, with rates of change ranging from 0.09 to 0.16 ºC decade^{-1} (0.07 to 0.13 ºC decade^{-1}) and from 0.17 to 0.39 ºC decade^{-1} (0.13 to 0.29 ºC decade^{-1}) for RCP 2.6 and 6.0 respectively. These warming rates are consistent with the increase in the air temperature, with rates of change ranging from 0.10 to 0.18 ºC decade^{-1} (0.08 to 0.15 ºC decade^{-1}) for RCP 2.6 and from 0.20 to 0.44 ºC decade^{-1} (0.15 to 0.33 ºC decade^{-1}) for RCP 6.0. For RCP 2.6 HadGEM2-ES projected the largest increases in surface temperature of 1.48 ºC (1.20 ºC), whereas for RCP 6.0 IPSL-CM5A-LR and HadGEM2-ES both projected similar large increases in surface temperature of 3.59 ºC (2.66 ºC) and 3.52 ºC (2.58 ºC) respectively. Significant rates of change in bottom temperature were not predicted during the RCP 2.6 scenario, but for the RCP 6.0 scenario bottom temperature did undergone significant warming rates in most projections, ranging from 0.07 to 0.11 ºC decade^{-1}.

There were also projected changes in the resistance to mechanical mixing. For RCP 2.6 rates of change in Schmidt stability were significant for IPSL-CMR5A-LR and HadGEM2-ES, corresponding to the same projections that experienced the largest increases in surface temperature, being 2.52 J m^{-2} decade^{-1} (1.87 J m^{-2} decade^{-1}) and 2.60 J m^{-2} decade^{-1} (2.21 J m^{-2} decade^{-1}) respectively. For RCP 6.0 a significant rate of change was projected in all projections, ranging from 2.50 to 7.93 J m^{-2} decade^{-1} (1.89 to 6.14 J m^{-2} decade^{-1}). For RCP 2.6 a significant rate of change in the duration of stratification was projected to be 1.73 and 1.01 days decade^{-1} (1.37 and 0.80 day decade^{-1}), which increased the stratification period by 16 and 9 days (13 and 7 days) for IPSL-CM5A-LR and HadGEM2-ES projections respectively. This resulted from changes in both the onset and loss of stratification (Table 5). For RCP 6.0, there was a further rate of change in the duration of stratification from 2.19 to 3.55 day decade^{-1} (1.78 to 2.94 day decade^{-1}), which resulted in a 20 to 33 days (17 to 27 days) longer stratification period. Thermocline depth is expected to be shallower under future conditions. However, for RCP 2.6 significant rates of change were not simulated, but for RCP 6.0 significant rates of change were found to be 0.08 and 0.12 m decade^{-1} (0.08 and 0.12 m decade^{-1}) or rather 0.74 and 1.13 m shallower (0.78 and 1.14 m) for IPSL-CM5A-LR and HadGEM2-ES.

Extreme changes also showed a pronounced increase during the future scenarios. For the RCP 6.0 scenario, the 95th percentile from the distribution of surface temperature anomalies ranged from 2.46 ºC (1.87 ºC) for GFDL-ESM2M to 5.02 ºC (3.76 ºC) for HadGEM2-ES (Fig. 5). The HadGEM2-ES projection also showed the highest increase in stability, 95th percentile of 112.51 J m^{-2} (89.05 J m^{-2}), and the shallowest thermocline depth, 95th percentile of 1.99 m (1.78 m). Extreme changes in the duration of stratification were least for GFDL-ESM2 and greatest for HadGEM2-ES. Longer stratification periods were projected for both models with the 95th percentile of change in duration increasing 51 days (38 days) for HadGEM2-ES and 22 days (21 days) GFDL-ESM2M projection. These increases in duration were dominated by earlier onset of stratification for GFDL-ESM2M and by both earlier onset and later fall overturn for HadGEM2-ES (Table 5).

4. Discussion

The GOTM model was able to produce a good agreement between the model output and observed data during both the calibration and the validation period (Fig. 3, Table 4). Water temperature simulations for the validation period (2015-2016)

https://doi.org/10.5194/hess-2019-335
Preprint. Discussion started: 8 July 2019


Hydrology and Earth System Sciences
Discussions

were more accurate than for the calibration period (2006-2014) due the higher variability in observed water temperature during the long calibration period. Bottom water temperature RMSEs showed better agreement between simulations and observations when the lake model was forced using measured average hourly meteorological data instead of measured average daily meteorological data. This could be attributed to a more confident prediction of the diurnal heating and cooling cycles, and hence the downward flow of heat into the hypolimnion. Thermocline depth was harder to predict, simulated thermocline depths differed from the observed values contributing to additional errors in water temperature for depths near the thermocline. Bruce et al. (2018) detected a strong correlation between accuracy of the extinction coefficient and model simulations of full-profile temperature and thermocline depth, and thus the importance of light extinction in the prediction of thermocline depth. A single calibrated value of e-folding depth for the visible fraction of the light (the inverse of the extinction coefficient) were used in the GOTM which prevented the evaluation of seasonal effects (Perroud et al., 2009). Also it should be noted that the internal seiche movement observed in the measured data (Fig. 2) is not simulated by a 1D model such as GOTM. Thus errors in thermocline depth are at least in part due to limitations in the 1D model framework.

The performance of the GOTM model are comparable to those reported in other 1-D modelling studies. Moras et al. (2019, in review) ran GOTM using hourly measured meteorology for a 56-year period and RMSE for daily full-profile water temperature was 1.12 ºC, Magee and Wu (2017) reported RMSEs of 0.30 and 0.53ºC (lake Mendota) and 1.45 and 1.94 ºC (Fish lake) for DYRESM temperature simulations in the epilimnion and hypolimnion respectively, and Perroud et al. (2009) simulated water temperature profiles of lake Geneva for a 10-year period with RMSEs of < 2 ºC for DYRESM and 3 ºC for SIMSTRAT. For our simulations with GOTM, model performance was slightly more accurate for the calibration data set when GOTM was forced with synthetic hourly meteorological input, rather than measured hourly meteorological input. Similar levels of performance using the two different data sets was in part caused by changes in the calibrated parameters used to characterize the lake thermal structure. Apparently calibration can in part compensate for the lack of diurnal variability in the daily forcing data.

The model parameters adjusted during the calibration processes were nondimensional scaling factors (shf_factor, swr_factor and wind_factor) and physical parameters with strong influence in the vertical distribution of light and temperature (k_min and g2). These parameters are key for the determination of the heat budget in the water column. Wind is the dominant driver of mixing in lakes, increases or decreases of wind speed (wind_factor) changes the amount of turbulence kinetic energy available for mixing. The wind scaling factor is often important when wind station is located some distance from the lake and/or to consider wind sheltering effects (Markfort et al., 2010). One would not expect that these factors would be important for Lake Erken where wind was measured on an island in the lake. However, the dominant wind along the lake's longest east-west fetch (Yang et al., 2014), this could explain the need to scale up the unidirectional wind speed measurements that were used as an input to GOTM. Furthermore, since it is the cube of wind speed that affects lake mixing, use of longer averaging periods will underestimate the effects of gusting and variable winds. This could explain why we obtain higher calibrated values of the wind factor when forcing the model with measured daily rather than hourly data (Table 2). Higher values of the wind_factor were also obtained when GOTM was forcing with synthetic hourly meteorological

https://doi.org/10.5194/hess-2019-335
Preprint. Discussion started: 8 July 2019


Hydrology and Earth System Sciences
Discussions

drivers. This is due to an underestimation of the faster wind speed predictions from GRNN model (Fig. 1, supplementary Fig. 5). During the ACPy calibration each of these parameters were calibrated while simultaneously influencing each other; shf_factor, swr_factor, wind_factor and g2 have a strong influence on heat and energy exchange across the air-water interface. There is to some extent an unavoidable tendency for some error in one parameter to be cancelled out by opposite errors in another parameter. When GOTM was forcing with measured daily average and synthetic hourly meteorological drivers a large wind_factor led to surface cooling, but on the other hand a lower shf_factor and smaller values of g2 (equivalent to higher extinction coefficient) promoted an increase in surface water temperature. When GOTM was forcing with measured hourly average meteorological drivers, g2 had the larger values (equivalent to lower extinction coefficient) and shf_factor was closer to 1 showing that a deeper penetration of energy entering into the lake provided more realistic warming of the surface, a lower wind factor was also found, which means that less surface cooling is to be offset.

In general, surface water temperature was projected to increase at a rate that is 83-93 % of that of the air temperature increase. This conclusion is in close agreement with other modelling studies which found a relationship between the surface water and air warming rates of 75-90% (Schmidt et al., 2014) and 70-85% (Shatwell et al., 2019). However, one exception was observed for the IPSL-CM5A-LR projection under RCP 2.6 scenario using daily resolution in the forcing inputs when increase of 0.109 ºC decade^{-1} in surface water temperature slightly exceeded the increase of 0.105 ºC decade^{-1} in air temperature. The reasons for that this scenario shows a somewhat different behaviour is probably related to some inconsistencies in the GCM models and also bias correction that was applied to the ISIMIP data.

4. Conclusion

This study showed the ability of the GOTM model to simulate accurately Lake Erken water temperature when the model was forced using either daily or hourly temporal resolution inputs. Neuronal networks were shown to be an effective method to disaggregate different weather variables such as air temperature, and short-wave radiation, in order to generate synthetic hourly meteorological data from the daily data that is typically available from GCM models. Model performance was slightly improved when using the synthetic hourly data, and climate change effects were somewhat greater when using such data to drive future climate simulations. However, it is not clear that data disaggregation is needed given the computational costs of developing such data sets and running long-term simulations at an hourly time step. Future climate simulations showed similar trends in the anomaly distributions when the GOTM model was forced with both mean daily or synthetic hourly meteorological data, and we also found evidence that the calibration procedure partly compensates for differences in the temporal resolution of the model input.

In this study changes in Lake Erken's surface temperature was projected to increase from 0.87 to 1.48 ºC for RCP 2.6 and from 1.59 to 3.59 for RCP 6.0, and the length of the stratification also was projected to be longer from 9 to 16 days for RCP 2.6 and from 20 to 33 days for RCP 6.0. We also extensively document coinciding changes in water column temperatures, water column stability and mixed layer depth both in this paper and the supplementary material. Combined these results suggest important changes in the factors affecting lake biogeochemistry directly through changes in temperature and

https://doi.org/10.5194/hess-2019-335
Preprint. Discussion started: 8 July 2019


Hydrology and Earth System Sciences
Discussions

indirectly by influencing the availability of light and nutrients. By providing an initial test for the simulations that will be carried out by the ISIMIP lake sector this paper sets the stage for more extensive world-wide evaluation of the effects of climate change on lake thermal structure.

Code and data availability

The source code of the model GOTM is freely available online at https://gotm.net/. The input data, model configuration, output and observed data for calibration are stored in HydroShare at https://doi.org/10.4211/hs.ace98c3bc72b44f1834a58ec8b3af310. The ISIMIP climate scenarios are available online at https://www.isimip.org/. Future projections of simulated water temperature derived from both the original ISIMIP input data and synthetic hourly projections are stored in HydroShare at https://doi.org/10.4211/hs.2b4cfe0f02bf4375bcd0b62e45c61b19. Matlab codes, R codes and all the datasets produced during this study are available upon request from the corresponding author.

Competing interests

The authors declare that they have no conflict of interest.

Acknowledgements

We are grateful to ISIMIP for their roles in producing, coordinating, and making available the ISIMIP climate scenarios, we acknowledge the support of the ISIMIP cross sectoral science team. We acknowledge funding from the EU and FORMAS in the frame of the collaborative international Consortium PROGNOS financed under the ERA-NET WaterWorks2014 Cofunded Call. This ERA-NET is an integral part of the 2015 Joint Activities developed by the Water Challenges for a Changing World Joint Programme Initiative (Water JPI). We also acknowledge funding from the European Union's Horizon 2020 research and innovation programme under the Marie Sklodowska-Curie grant agreement H2020-MSCA-ITN-2016 No 722518 for the Project MANTEL, and the project WATExR which is part of ERA4CS, an ERA-NET initiated by JPI Climate, and funded by MINECO (ES),FORMAS (SE), BMBF (DE), EPA (IE), RCN (NO), and IFD (DK),with co-funding by the European Union (Grant 690462) and FORMAS grant 2017-01738.

References

Bruce, L. C., Frassl, M. A., Arhonditsis, G. B., Gal, G., Hamil-ton, D. P., Hanson, P. C., Hetherington, A. L., Melack, J. M.,Read, J. S., Rinke, K., Rigosi, A., Trolle, D., Winslow, L., Adrian, R., Ayala, A. I., Bocaniov, S. A., Boehrer, B., Boon, C.,Brookes, J. D., Bueche, T., Busch, B. D., Copetti, D., Cortés,A., de Eyto, E., Elliott, J.A., Gallina, N., Gilboa, Y., Guyen-non, N., Huang, L., Kerimoglu, O., Lenters, J.D., MacIntyre, S.,Makler-Pick, V., McBride, C. G., Moreira, S., Özkundakci, D.,Pilotti, M., Rueda, F. J., Rusak, J. A., Samal, N. R., Schmid, M.,Shatwell, T., Snorthheim, C., Soulignac, F., Valerio, G., van derLinden, L., Vetter, M., Vinçon-Leite, B., Wang, J., Weber, M.,Wickramaratne, C., Woolway, R. I., Yao, H., and

Hipsey, M. R.: A multi-lake comparative analysis of the General Lake Model(GLM): Stress-testing across a global observatory network, Environ. Modell. Softw., 102, 274–291, https://doi.org/10.1016/j.envsoft.2017.11.016, 2018.

Bruggeman, J., and Bolding, K.: A general framework for aquatic biogeochemical models, Environ. Model Softw., 61, 249–265, https://doi.org/10.1016/j.envsoft.2014.04.002, 2014.

Burchard, H., Bolding, K., and Ruiz-Villarreal, M.: GOTM, a General Ocean Turbulence Model. Theory, implementation and test cases, Technical Report, 1999.

Butcher, J. B., Nover, D., Johnson, T. E., and Clark, C. M.: Sensitivity of lake thermal and mixing dynamics to climate change, Clim. Change, 129, 295-305, https://doi.org/10.1007/s10584-015-1326-1, 2015.

Frieler, K., Lange, S., Piontek, F., Reyer, C. P. O., Schewe, J., Warszawski, L., Zhao, F., Chini, L., Denvil, S., Emanuel, K., Geiger, T., Halladay, K., Hurtt, G., Mengel, M., Murakami, D., Ostberg, S., Popp, A., Riva, R., Stevanovic, M., Suzuki, T., Volkholz, J., Burke, E., Ciais, P., Ebi, K., Eddy, T. D., Elliott, J., Galbraith, E., Gosling, S. N., Hattermann, F., Hickler, T., Hinkel, J., Hof, C., Huber, V., Jägermeyr, J., Krysanova, V., Marcé, R., Müller Schmied, H., Mouratiadou, I., Pierson, D., Tittensor, D. P., Vautard, R., van Vliet, M., Biber, M. F., Betts, R. A., Bodirsky, B. L., Deryng, D., Frolking, S., Jones, C. D., Lotze, H. K., Lotze-Campen, H., Sahajpal, R., Thonicke, K., Tian, H., and Yamagata, Y.: Assessing the impacts of 1.5 °C global warming – simulation protocol of the Inter-Sectoral Impact Model Intercomparison Project (ISIMIP2b), Geosci. Model Dev., 10, 4321-4345, https://doi.org/10.5194/gmd-10-4321-2017, 2017.

Ficker, H., Luger, M., and Gassner, H.: From dimictic to monomictic: Empirical evidence of thermal regime transitions in three deep alpine lakes in Austria induced by climate change, Fresh. Biol., 62, 1335-1345, https://doi.org/10.1111/fwb.12946, 2017.

Foley, B., Jones, I.D., Maberly, S.C., and Rippey, B.: Long-term changes in oxygen depletion in a small temperate lake: effects of climate change and eutrophication. Freshwater Biol., 57, 278-289, https://doi.org/10.1111/j.1365-2427.2011.02662.x, 2012.

Grasset, C., Mendonça, R., Villamor Saucedo, G., Bastviken, D., Roland, F., and Sobek, S.: Large but variable methane production in anoxic freshwater sediment upon addition of allochthonous and autochthonous organic matter, Limnol. Oceanogr., 63, 1488-1501, https://doi.org/10.1002/lno.10786, 2018.

Guo, Z., Chang, C., Wang, R.: A Novel Method to Downscale Daily Wind Statistics to Hourly Wind Data for Wind Erosion Modelling, in: Geo-Informatics in Resource Management and Sustainable Ecosystem, GRMSE 2015, Wuhan, China, 16-18 October 2015, 611-619, 2015.

Hadley, K. R., Paterson, A. M. , Stainsby, E. A., Michelutti , N. , Yao, H. , Rusak, J. A., Ingram, R., McConnell, C., and Smol, J. P.: Climate warming alters thermal stability but not stratification phenology in a small north-temperature lake, Hydrol. Process., 28, 6309-6319, https://doi.org/10.1002/hyp.10120, 2013.

Hempel, S., Frieler, K., Warszawski, L., Schewe, J., and Piontek, F.: A trend-preserving bias correction – the ISI-MIP approach, Earth Syst. Dynam., 4, 219-236, https://doi.org/10.5194/esd-4-219-2013, 2013.

Huang, Y. T., and Liu, L.: Multiobjective water quality model calibration using a hybrid genetic algorithm and neural network-based approach, J. Environ. Eng., 136, 1020-1031, https://doi.org/10.1061/(ASCE)EE.1943-7870.0000237, 2010.

Kainz, M. J., Ptacnik, R., Rasconi, S., and Hager, H. H.: Irregular changes in lake surface water temperature and ice cover in subalpine Lake Lunz, Austria, Inland Waters, 7, 27-33, http://dx.doi.org/10.1080/20442041.2017.1294332, 2017.

Khatib, T., and Elmenreich, W.: A Model for Hourly Solar Radiation Data Generation from Daily Solar Radiation Data Using a Generalized Regression Artificial Neural Network, Int. J. Photoenergy, 968024,1–13, https://doi.org/10.1155/2015/968024, 2015.

Kirillin, G.: Modeling the impact of global warming on water temperature and seasonal mixing regimes in small temperate lakes. Boreal Enviro. Res., 15, 279-293, 2010.

Kraemer, B. M., Anneville, O., Chandra, S., Dix, M., Kuusisto, E., Livingstone, D. M., Rimmer, A., Schladow, S. G., Silow, E., Sitoki, L. M., Tamatamah, R., Vadeboncoeur, Y., and McIntyre, P. B.: Morphometry and average temperature affect lake stratification responses to climate change, Geophys. Res. Lett., 42, 4981–4988, https://doi.org/10.1002/2015GL064097, 2011.

Ladwig, R., Furusato, E., Kirillin, G., Hinkelmann, R., and Hupfer, M.: Climate change demands adaptative management of urban lakes: model-based assessment of management scenarios for lake Tegel (Berlin, Germany), Water, 10, 186, https://doi.org/10.3390/w10020186, 2018.

MacKay, M. D., Neale, P. J., Arp, C. D., De Senarpont Domus, L. N., Fang, X., Gal, G., Jöhnk, K. D., Kirillin, G., Lenters, J. D., Litchman, E., MacIntyre, S., Marsh, P., Melack, J., Mooij, W. M., Peeters, F., Quesada, A., Schladow, S. G., Schmid, M., Spence, C., and Stokes, S. L.: Modeling lakes and reservoirs in the climate system, Limnol. Oceanogr., 54, 2315–2329, https://doi.org/10.4319/lo.2009.54.6_part_2.2315, 2009.

Magee, M. R., and Wu, C. H.: Response of water temperatures and stratification to changing climate in three lakes with different morphometry, Hydrol. Earth Syst. Sci., 21, 6253-6274, https://doi.org/10.5194/hess-21-6253-2017, 2017.

Markfort, C. D., Perez, A. L. S., Thill, J. W., Jaster, D. A., Porte-Agel, F., and Stefan, H. G.: Wind sheltering of a lake by a tree canopy or bluff topography. Water Resour. Res. 46, 1-13, https://doi.org/10.1029/2009WR007759, 2010.

Mesman, J. P., Stelzer, J. A. A., Dakos, V., Goyette, S., Jones, I. D., Kasparian, J., McGinnis, D. F., and Ibelings, B. W.: The role of internal feedbacks in shifting deep lake mixing regimes under a warming climate, submitted to Glob. Chang. Biol., 2019.

Moras, S., Ayala, A. I., and Pierson, D. C.: Historical modelling of changes in Lake Erken thermal conditions, Hydrol. Earth Syst. Sci. Discuss., https://doi.org/10.5194/hess-2019-199, in review, 2019.

Nash, J. E., and Sutcliffe, J. V.: River flow forecasting through conceptual models part I - A discussion of principles. J. Hydrol., 10, 282–290. https://doi.org/10.1016/0022-1694(70)90255-6, 1970.

Nõges, T., Nõges, P., Jolma, A., and Kaitaranta, J.: Impacts of climate change on physical characteristics of lakes in Europe. European Commission Joint Research Centre Report EUR 24064 EN, Office for Official Publications of the European Communities, Luxembourg, 2009.

North, R. P., North, R. L., Livingstone, D. M., Köster, O., and Kipfer, R.: Long-term changes in hypoxia and soluble reactive phosphorus in the hypolimnion of a large temperate lake: consequences of a climate regime shift. Glob. Chang. Biol., 20, 811-823, https://doi.org/10.1111/gcb.12371, 2013.

O'Reilly, C., Sharma, S., Gray, D. K., Hampton, S. E., Read, J. S., Rowle,y R. J., Schneider, P., Lenters, J. D., McIntyre, P.B., Kraemer, B. M., Weyhenmeyer, G. A., Straile, D., Dong, B., Adrian, R., Allan, M. G., Anneville, O., Arvola, L., Austin, J., Bailey, J. L., Baron, J. S., Brookes, J. D., de Eyto, E., Dokulil, M. T., Hamilton, D. P., Havens, K., Hetherington, A. L., Higgins, S. N., Hook, S., Izmest'eva, L. R., Joehnk, K. D., Kangur, K., Kasprzal, P., Kumagai, M., Kuusisto, E., Leshkevich, 20 G., Livingtone, D. M., McIntyre, S., May, L., Melack, J. M., Mueller-Navarra, D. C, Naumenko, M., Noges, P., Noges, T., North, R. P., Plisnier, P. D., Rigosi, A., Rimmer, A., Rogora, M., Rudstam, L. G., Rusak, J. A., Salmaso, N., Samal, N. R., Schindler, D. E., Schladow, S. G., Schmid, M., Schmidt, S. R., Silow, E., Soylu, M. E., Teubner, K., Verburg, P., Voutilainen, A., Watkinson, A., Wiliamson, C. E., and Zhang G.: Rapid and highly variable warming of lake surface waters around the globe, Geophys. Res. Lett., 42, 10773–10781, https://doi.org/10.1002/2015GL066235, 2015.

Shimoda, Y., Azim, M.E., Perhar, G., Ramin, M., Kenney, M.A., Sadraddini, S., Gudimov, A., and Arhonditsis, G.B.: Our current understanding of lake ecosystem response to climate change: What have we really learned from the north temperate deep lakes?, J. Great Lakes Res., 37, 173-193, https://doi.org/10.1016/j.jglr.2010.10.004, 2011.

O'Reilly, C. M., Alin, S. R., Plisnier, P. D., Cohen, A. S., and McKee, B. A.: Climate change decreases aquatic ecosystem productivity of Lake Tanganyika, Africa, Nature, 424, 766-768, https://doi.org/10.1038/nature01833, 2003.

Parton, W. J., and Logan, J. A.: A model for diurnal variation in soil and air temperature, J. Agric. Meteorol., 23, 205-2016, 1981.

Pearl, H.W. and Paul, V.J.: Climate change: links to global expansion of harmful cyanobacteria. Water Res., 46, 1349-1363, https://doi.org/10.1111/j.1758-2229.2008.00004.x, 2012.

Perroud, M., and Goyette, S.: Impact of warmer climate on Lake Geneva water-temperature profiles, Boreal Environ. Res., 15, 255-278, 2010.

Perroud, M., Goyette, S., Martynov, A., Beniston, M., and Anneville, O.: Simulation of multiannual thermal profiles in deep Lake Geneva: A comparison of one-dimensional lake models, Limnol. Oceanogr., 54, 1574-1594, https://doi.org/10.4319/lo.2009.54.5.1574, 2009.

Persson, I., and Jones, I.D.: The effect of water colour on lake hydrodynamics: A modelling study, Freshwater Biol., 53, 2345-2355, https://doi.org/10.1111/j.1365-2427.2008.02049.x, 2008.

Pierson, D. C., Petterson, K., and Istvanovics, V.: Temporal changes in biomass specific photosynthesis during the summer: regulation by environmental factors and the importance of phytoplankton succession, Hydrobiologia, 243, 119-135, 1992.

Read, J. S., Hamilton, D. P., Jones, I. D., Muraoka, K., Winslow, L. A., Kroiss, R., Wu, C. H., and Gaiser, E.: Derivation of lake mixing and stratification indices from high-resolution lake buoy data, Environ. Model Softw., 26 1325-1336, https://doi.org/10.1016/j.envsoft.2011.05.006, 2011.

Rempfer, J., Livingstone D. M., Blodau, C., Niederhauser, P., Forster R., and Kipfer, R.: The effect of the exceptionally mild European winter of 2006–2007 on temperature and oxygen profiles in lakes in Switzerland: a foretaste of the future?, Limnol. Oceanogr., 55, 2170–2180, https://doi.org/10.4319/lo.2010.55.5.2170, 2010.

Sachse, R., Petzoldt, T., Blumstock, M., Moreira Martinez, S., Pätzig, M., Rücker, J., Janse, J., Mooij, W. M., and Hilt, S.: Extending one-dimensional models for deep lakes to simulate the impact of submerged macrophytes on water quality, Environ. Model Softw., 61, 410–423, https://doi.org/10.1016/j.envsoft.2014.05.023, 2014.

Sahoo, G. B., Forrest, A. L., Schladow, S. G., Reuter, J. E., Coats, R., and Dettinger, M.: Climate change impacts on lake thermal dynamics and ecosystem vulnerabilities, Limnol. Oceanogr., 61, 496-507, https://doi.org/10.1002/lno.10228, 2019.

Samal, N. R., Pierson, D. C., Schneiderman, E., Huang, Y., Read, J. S., Anandhi, A., and Owens, E. M.: Impact of climate change on Cannonsville Reservoir thermal structure in the New York City water supply, Water Qual. Res. J. Can., 47, 389-405, https://doi.org/10.2166/wqrjc.2012.020, 2010.

Schmid, M., Hunziker, S. and Wüest, A.: Lake surface temperatures in a changing climate: a global sensitivity analysis, Clim. Change, 124, 301-315. https://doi.org/10.1007/s10584-014-1087-2, 2014.

Schultze, M., Boehrer, B., Wendt-Potthoff, K., Katsev, S., and Brown, E. T.: Chemical Setting and Biogeochemical Reactions in Meromictic Lakes. Ecology of Meromictic Lakes, Springer, 35-59 pp., 2017.

Schwefel, R., Gaudard, A., Wüest, A., and Bouffard, D.: Effects of climate change on deepwater oxygen and winter mixing in a deep lake (Lake Geneva): Comparing observational findings and modeling. Water Resour. Res., 52, 8811-8826, https://doi.org/10.1002/2016WR019194, 2016.

Sen, P. K.: Estimates of the regression coefficient based on Kendall's Tau, J. Am. Stat. 5 Assoc., 63, 1379–1389, https://doi.org/10.1080/01621459.1968.10480934, 1968.

Shatwell, T., Thiery, W., and Kirillin, G.: Future projections of temperature and mixing regime of European temperate lakes, Hydrol. Earth Syst. Sci., 23, 1533-1551, https://doi.org/10.5194/hess-23-1533-2019, 2019.

Storn, R., and Price K.: Differential Evolution – A Simple and Efficient Heuristic for Global Optimization over Continuous 10 Spaces, J. Global Optim., 11, 341–359, https://doi.org/10.1023/A:1008202821328, 1997.

Theil, H.: A rank invariant method of linear and polynomial regression analysis, I, II, III, Proc. K. Ned. Akad. Wet., Ser. A Math. Sci., 53, 386–392, 1950.

Umlauf, L., and Burchard, H.: Second-order turbulence closure models for geophysical boundary layers. A review of recent work. Continental Shelf Research, 25,795–827. https://doi.org/10.1016/j.csr.2004.08.004, 2005.

Waichler, S. R., and Wigmosta, M. S.: Development of hourly meteorological values from daily data and significance to Hydrological Modeling at H. J. Andrews Experimental Forest, J. Hydrometeorol., 4, 251-263, https://doi.org/10.1175/1525-7541(2003)4<251:DOHMVF>2.0.CO;2, 2003.

Winslow, L. A., Hansen, G. J. A, Read J. S., and Notaro, M.: Large-scale modeled contemporary and future water temperature estimates for 10774 Midwestern U.S. Lakes, Sci. Data, https://doi.org/10.1038/sdata.2017.53, 2017.

https://doi.org/10.5194/hess-2019-335
Preprint. Discussion started: 8 July 2019

Woolway, R.I., and Merchant, C.J.: Worldwide alteration of lake mixing regimes in response to climate change. Nature Geoscience, 12, 271-276, https://doi.org/10.1038/s41561-019-0322-x, 2019.

Woolway, R. I., Meinson, P., Nõges, P., Jones, I. D., and Laas, A.: Atmospheric stilling leads to prolonged thermal stratification in a large shallow polymictic lake. Clim. Change, 141, 759-773, https://doi.org/10.1007/s10584-017-1909-0, 2017.

Yang, Y., Colom, W., Pierson, D. C, and Pettersson, K.: Water column stability and summer phytoplankton dynamics in a temperate lake (Lake Erken, Sweden), Inland Waters, 6, 499-508, https://doi.org/10.1080/IW-6.4.874, 2016.

Yankova, Y., Neuenschwander, S., Köster, O., and Posch, T.: Abrupt stop of deep water turnover with lake warming: Drastic consequences for algal primary producers. Sci. Rep., 7, 13770, https://doi.org/10.1038/s41598-017-13159-9, 2017.

Tables

Table 1: Bias-corrected variables in the ISIMIP dataset

variable name	abbreviation	units
precipitation	pr	kg m^{-2} s^{-1}
surface pressure	ps	Pa
surface downwelling shortwave radiation	rsds	W m^{-2}
near-surface wind speed	sfcWind	m s^{-1}
near-surface air temperature	tas	K
daily maximum near-surface air temperature	tasmax	K
daily minimum near-surface air temperature	tasmin	K
relative humidity	hurs	%

Table 2: Lake model parameters and calibrated values

model parameter	feasible range	calibrated values		
		24 h met	1h met	synthetic 1h met
shf_factor	0.5–1.5	0.69	0.81	0.77
swr_factor	0.8–1.2	1.15	0.90	0.91
wind_factor	0.5–2.0	1.55	1.37	1.51
k_min	1.4 10^{-7}–1.0 10^{-5}	1.47 10^{-6}	1.40 10^{-6}	1.29 10^{-6}
g2	0.5–3.5	1.99	2.30	1.62

https://doi.org/10.5194/hess-2019-335
Preprint. Discussion started: 8 July 2019

Hydrology and Earth System Sciences
Discussions

Table 3: GRNN models performance evaluation.

	training			validation		
GRNN model	MBE	RMSE	NSE	MBE	RMSE	NSE
Air temperature (ºC)	$-1.70\ 10^{-4}$	0.256	0.999	-0.057	0.318	0.940
Short wave radiation (W m^{-2})	$5.76\ 10^{-4}$	6.345	0.999	-0.037	8.196	0.870
Relative humidity (%)	$-7.94\ 10^{-4}$	0.790	0.998	0.341	1.021	0.686
Wind speed (m s^{-1})	$-5.67\ 10^{-3}$	1.060	0.779	-0.009	1.370	0.584

Table 4: Lake model performance evaluation: MBE, RMSE and NSE for full profiles temperature, surface temperature, bottom temperature, volumetrically weighted averaged whole lake temperatures, Schmidt stability and thermocline using simulated results from running GOTM driven by daily (24h met), hourly (1h met) and synthetic hourly (synthetic 1h met) meteorological data sets.

	calibration								
	24h met			1h met			synthetic 1h met		
	MBE	RMSE	NSE	MBE	RMSE	NSE	MBE	RMSE	NSE
full-profile temp (ºC)	-0.08	1.04	0.93	-0.02	0.94	0.94	-0.02	0.88	0.95
surface temp (ºC)	-0.04	0.69	0.97	0.04	0.72	0.97	-0.01	0.61	0.98
bottom temp (ºC)	-0.06	1.33	0.83	0.07	1.24	0.85	-0.11	1.16	0.87
whole lake temp (ºC)	-0.07	0.57	0.98	-0.03	0.52	0.98	-0.01	0.49	0.98
Schmidt stability (J m^{-2})	0.53	22.09	0.85	0.59	21.69	0.85	0.76	19.64	0.88
thermocline depth (m)	0.58	2.77	0.32	0.84	3.07	0.22	0.43	2.84	0.32
	validation								
	24h met			1h met			synthetic 1h met		
	MBE	RMSE	NSE	MBE	RMSE	NSE	MBE	RMSE	NSE
full-profile temp (ºC)	-0.07	0.63	0.98	-0.12	0.69	0.97	0.00	0.68	0.97
surface temp (ºC)	-0.24	0.54	0.99	-0.19	0.64	0.98	-0.15	0.54	0.99
bottom temp (ºC)	0.16	0.68	0.96	0.09	0.59	0.97	0.23	0.74	0.95
whole-lake temp (ºC)	-0.13	0.48	0.99	-0.17	0.59	0.98	-0.06	0.51	0.98
Schmidt stability (J m^{-2})	-5.26	13.27	0.90	-3.26	13.50	0.90	-4.47	13.26	0.90
thermocline depth (m)	0.89	2.86	0.07	1.07	3.27	-0.07	0.98	3.18	-0.14

https://doi.org/10.5194/hess-2019-335
Preprint. Discussion started: 8 July 2019

Hydrology and Earth System Sciences
Discussions

Table 5. Projected trends of change (2006–2099) in air temperature, surface temperature, bottom temperature, whole-lake temperature, Schmidt stability, thermocline depth, duration, onset and loss of stratification (ns: not significant).

	RCP 2.6	
	GFDL-ESM2M	
	24 h met	1h met
air temperature	ns	ns
surface temperature	ns	ns
bottom temperature	ns	ns
whole-lake temperature	ns	ns
Schmidt stability	ns	ns
thermocline depth	ns	ns
duration	ns	ns
onset	ns	ns
loss	ns	ns
	HadGEM2-ES	
	24 h met	1h met
air temperature	0.18 ºC decade^{-1} (p-value < 0.001)	0.15 ºC decade^{-1} (p-value < 0.001)
surface temperature	0.16 ºC decade^{-1} (p-value < 0.001)	0.13 ºC decade^{-1} (p-value < 0.001)
bottom temperature	ns	ns
whole-lake temperature	0.10 ºC decade^{-1} (p-value < 0.001)	0.08 ºC decade^{-1} (p-value < 0.001)
Schmidt stability	2.60 J m^{-2} decade^{-1} (p-value < 0.001)	2.21 J m^{-2} decade^{-1} (p-value < 0.001)
thermocline depth	ns	ns
duration	1.01 day decade^{-1} (p-value = 0.014)	0.80 day decade^{-1} (p-value = 0.034)
onset	0.63 day decade^{-1} (p-value = 0.047)	ns
loss	ns	0.43 day decade^{-1} (p-value = 0.015)
	IPSL-CM5A-LR	
	24 h met	1h met
air temperature	0.11 ºC decade^{-1} (p-value = 0.005)	0.09 ºC decade^{-1} (p-value = 0.004)
surface temperature	0.11 ºC decade^{-1} (p-value = 0.003)	0.08 ºC decade^{-1} (p-value = 0.004)
bottom temperature	ns	ns
whole-lake temperature	0.06 ºC decade^{-1} (p-value = 0.038)	0.05 ºC decade^{-1} (p-value = 0.049)
Schmidt stability	2.52 J m^{-2} decade^{-1} (p-value = 0.012)	1.87 J m^{-2} decade^{-1} (p-value = 0.024)
thermocline depth	ns	ns
duration	1.73 day decade^{-1} (p-value < 0.001)	1.37 day decade-1 (p-value = 0.002)
onset	ns	0.93 day decade^{-1} (p-value = 0.004)
loss	0.85 day decade^{-1} (p-value = 0.005)	0.45 day decade^{-1} (p-value = 0.049)
	MIROC5	
	24 h met	1h met

https://doi.org/10.5194/hess-2019-335
Preprint. Discussion started: 8 July 2019

Hydrology and Earth System Sciences
Discussions

air temperature	0.10 ºC decade^{-1} (p-value = 0.007)	0.08 ºC decade^{-1} (p-value = 0.008)
surface temperature	0.09 ºC decade^{-1} (p-value = 0.001)	0.07 ºC decade^{-1} (p-value = 0.002)
bottom temperature	ns	ns
whole-lake temperature	0.08 ºC decade^{-1} (p-value < 0.001)	0.06 ºC decade^{-1} (p-value < 0.001)
Schmidt stability	ns	ns
thermocline depth	ns	ns
duration	ns	ns
onset	ns	0.60 day decade^{-1} (p-value = 0.018)
loss	ns	ns
	RCP 6.0	
	GFDL-ESM2M	
	24 h met	1h met
air temperature	0.20 ºC decade^{-1} (p-value < 0.001)	0.15 ºC decade-^{1} (p-value < 0.001)
surface temperature	0.17 ºC decade^{-1} (p-value < 0.001)	0.13 ºC decade^{-1} (p-value < 0.001)
bottom temperature	ns	ns
whole-lake temperature	0.15 ºC decade^{-1} (p-value < 0.001)	0.11 ºC decade^{-1} (p-value < 0.001)
Schmidt stability	2.50 J m^{-2} decade^{-1} (p-value = 0.003)	1.89 J m^{-2} decade^{-1} (p-value = 0.008)
thermocline depth	ns	ns
duration	ns	0.81 day decade^{-1} (p-value = 0.031)
onset	ns	ns
loss	ns	ns
	HadGEM2-ES	
	24 h met	1h met
air temperature	0.44 ºC decade^{-1} (p-value < 0.001)	0.33 ºC decade^{-1} (p-value < 0.001)
surface temperature	0.38 ºC decade^{-1} (p-value < 0.001)	0.28ºC decade^{-1} (p-value < 0.001)
bottom temperature	0.07 ºC decade^{-1} (p-value = 0.010)	ns
whole-lake temperature	0.25 ºC decade^{-1} (p-value < 0.001)	0.17 ºC decade^{-1} (p-value < 0.001)
Schmidt stability	7.79 J m^{-2} decade^{-1} (p-value < 0.001)	6.22 J m^{-2} decade^{-1} (p-value < 0.001)
thermocline depth	0.12 m decade^{-1} (p-value < 0.001)	0.12 m decade^{-1} (p-value < 0.001)
duration	3.55 day decade^{-1} (p-value < 0.001)	2.94 day decade^{-1} (p-value < 0.001)
onset	1.90 day decade^{-1} (p-value < 0.001)	1.41 day decade^{-1} (p-value < 0.001)
loss	1.80 day decade^{-1} (p-value < 0.001)	1.38 day decade^{-1} (p-value < 0.001)
	IPSL-CM5A-LR	
	24 h met	1h met
air temperature	0.43 ºC decade^{-1} (p-value < 0.001)	0.33 ºC decade^{-1} (p-value < 0.001)
surface temperature	0.39 ºC decade^{-1} (p-value < 0.001)	0.29 ºC decade^{-1} (p-value < 0.001)
bottom temperature	0.08 ºC decade^{-1} (p-value = 0.033)	ns
whole-lake temperature	0.27 ºC decade^{-1} (p-value < 0.001)	0.19 ºC decade^{-1} (p-value < 0.001)
Schmidt stability	7.93 J m^{-2} decade^{-1} (p-value < 0.001)	6.14 J m^{-2} decade^{-1} (p-value < 0.001)
thermocline depth	0.08 m decade^{-1} (p-value = 0.003)	0.08 m decade^{-1} (p-value < 0.001)

https://doi.org/10.5194/hess-2019-335
Preprint. Discussion started: 8 July 2019

duration	3.06 day decade^{-1} (p-value < 0.001)	2.39 day decade^{-1} (p-value < 0.001)
onset	1.87 day decade^{-1} (p-value < 0.001)	1.38 day decade^{-1} (p-value < 0.001)
loss	1.26 day decade^{-1} (p-value < 0.001)	1.02 day decade^{-1} (p-value < 0.001)
	MIROC5	
	24 h met	1h met
air temperature	0.32 ºC decade^{-1} (p-value < 0.001)	0.25 ºC decade^{-1} (p-value < 0.001)
surface temperature	0.28 ºC decade^{-1} (p-value < 0.001)	0.21ºC decade^{-1} (p-value < 0.001)
bottom temperature	0.11 ºC decade^{-1} (p-value < 0.001)	0.09 ºC decade^{-1} (p-value = 0.002)
whole-lake temperature	0.22 ºC decade^{-1} (p-value < 0.001)	0.17 ºC decade^{-1} (p-value < 0.001)
Schmidt stability	3.99 J m^{-2} decade^{-1} (p-value < 0.001)	2.77 J m^{-2} decade^{-1} (p-value = 0.005)
thermocline depth	ns	ns
duration	2.19 day decade^{-1} (p-value < 0.001)	1.78 day decade^{-1} (p-value < 0.001)
onset	1.71 day decade^{-1} (p-value = 0.002)	1.39 day decade^{-1} (p-value = 0.017)
loss	0.69 day decade^{-1} (p-value < 0.001)	0.43 day decade^{-1} (p-value < 0.001)

Figures

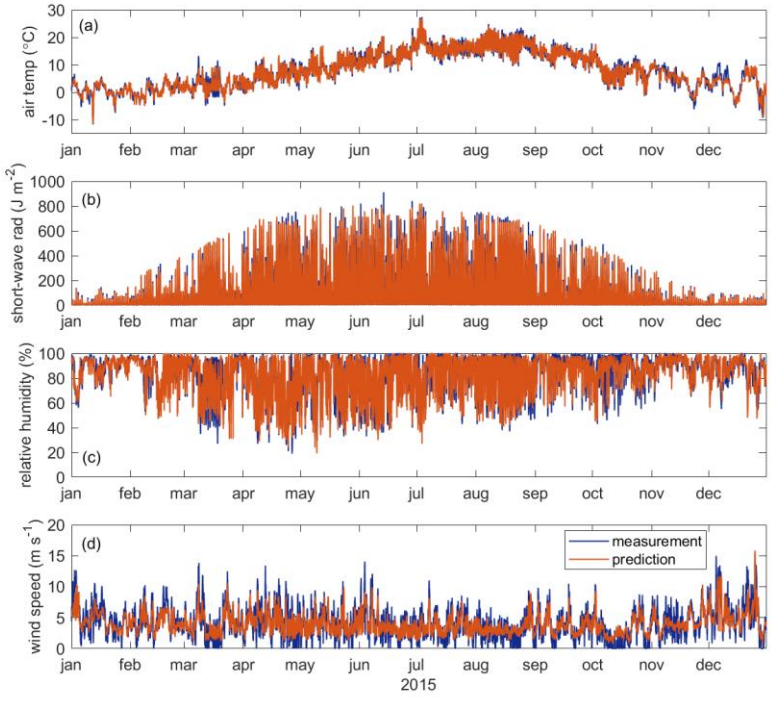

Figure 1. Measured vs predicted (a) air temperature, (b) short-wave radiation, (c) relative humidity and (d) wind speed for 2015 (validation data set).

550

https://doi.org/10.5194/hess-2019-335
Preprint. Discussion started: 8 July 2019

Hydrology and Earth System Sciences
Discussions

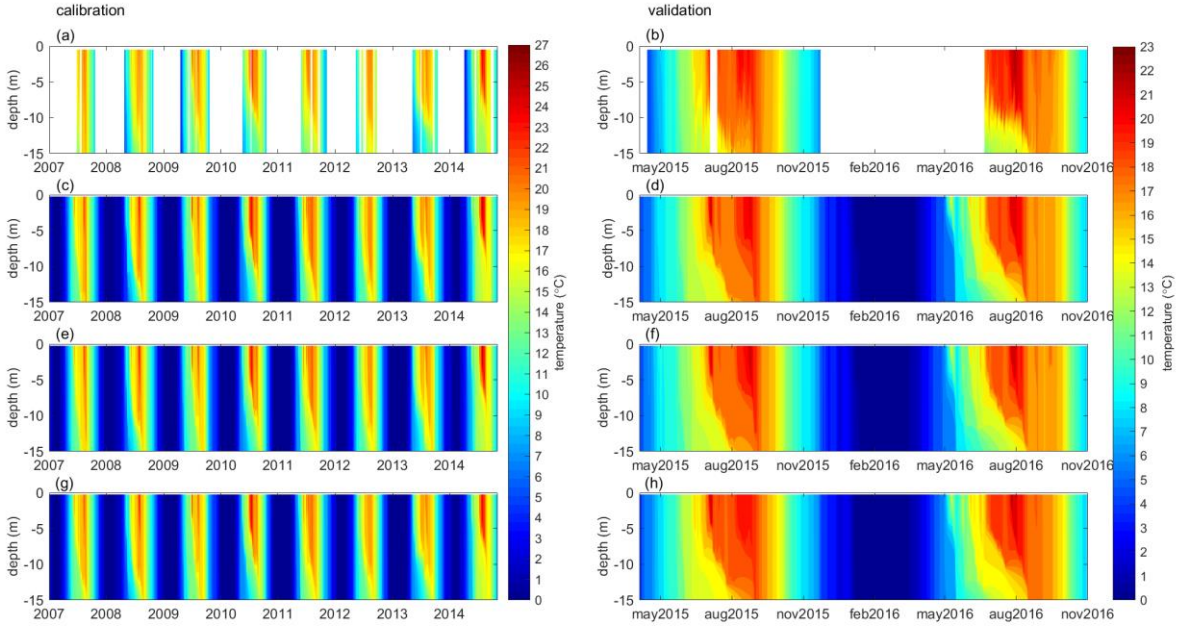

Figure 2. Daily averaged water temperature in Lake Erken for the validation (a)-(c)-(e)-(g) and calibration (b)-(d)-(f)-(h) periods: observations (a)-(b), simulations driven by daily meteorological data (c)-(d), hourly meteorological data (e)-(f) and synthetic hourly meteorological data (g)-(h).

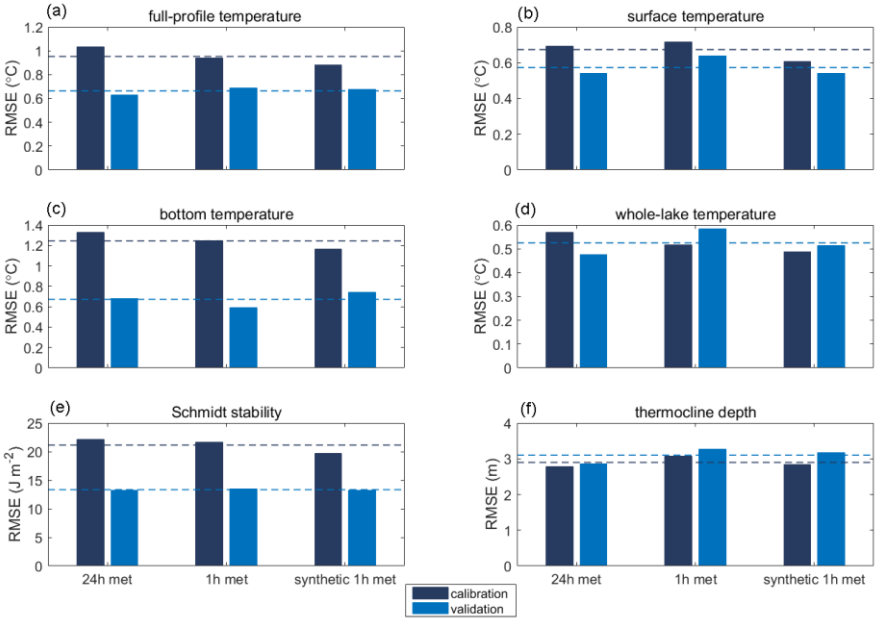

Figure 3. GOTM model performance metrics for prediction of (a) full-profile temperature which compared simulated and measured data at all possible depths, (b) surface temperature, (c) bottom temperature, (d) whole-lake temperature, (e) Schmidt stability and (f) thermocline depth. The mean (horizontal line) is also shown

https://doi.org/10.5194/hess-2019-335
Preprint. Discussion started: 8 July 2019

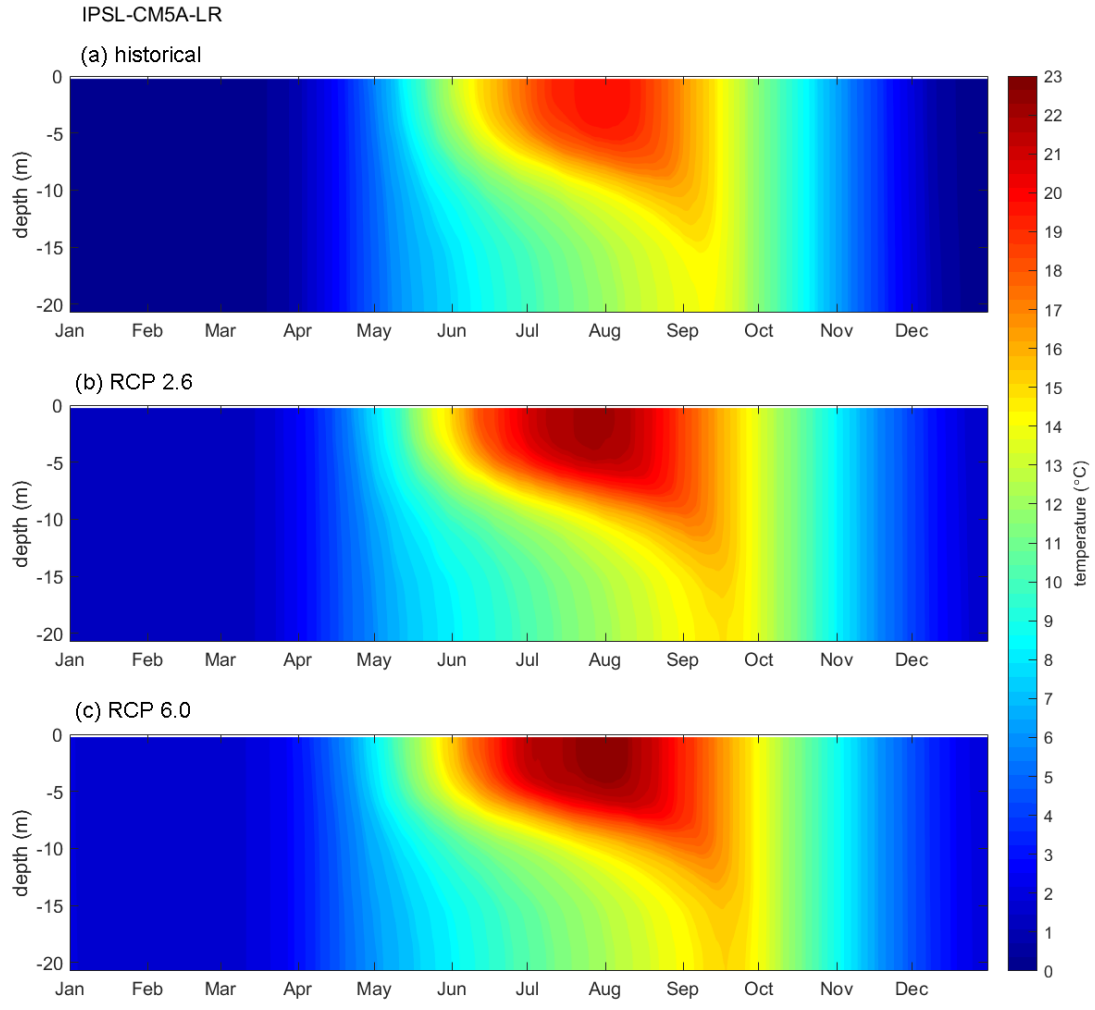

Figure 4. Temperature isopleth diagrams for the (a) historical, (b) RCP 2.6 and (c) RCP 6.0 scenarios showing results from the lake model forced with daily IPSL-CM5A-LR projections. The temperature matrix used to make these plots was created by averaging the simulated daily temperature profiles for every year in each scenario.

https://doi.org/10.5194/hess-2019-335
Preprint. Discussion started: 8 July 2019

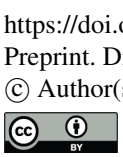

Hydrology and Earth System Sciences
Discussions
Open Access
EGU

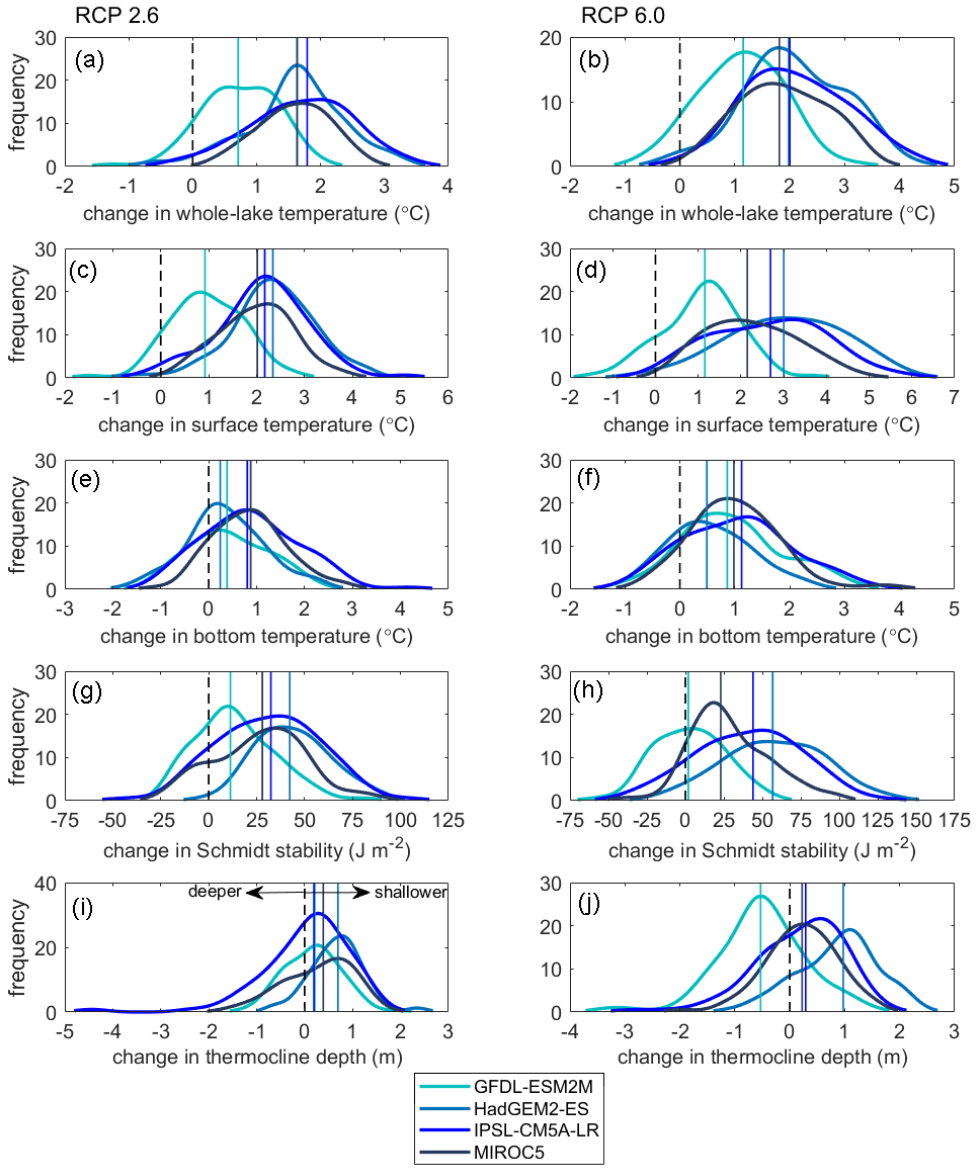

Figure 5. Changes in anomalies calculated from annually averaged (from April to September) (a)-(b) whole-lake temperature, (c)-(d) surface temperature, (e)-(f) bottom temperature, (g)-(h) Schmidt stability, (i)-(j) thermocline depth under (a)-(c)-(e)-(g)-(i) RCP 2.6 and (b)-(d)-(f)-(h)-(j) RCP 6.0, showing results from the lake model forced with daily GFDL-ESM2M, HadGEM2-ES, IPSL-CM5A-LR and MIROC5 projections. All changes are for 2006-2099 relative to 1975-2005. The median (vertical line) is also shown.

https://doi.org/10.5194/hess-2019-335
Preprint. Discussion started: 8 July 2019

Hydrology and Earth System Sciences
Discussions

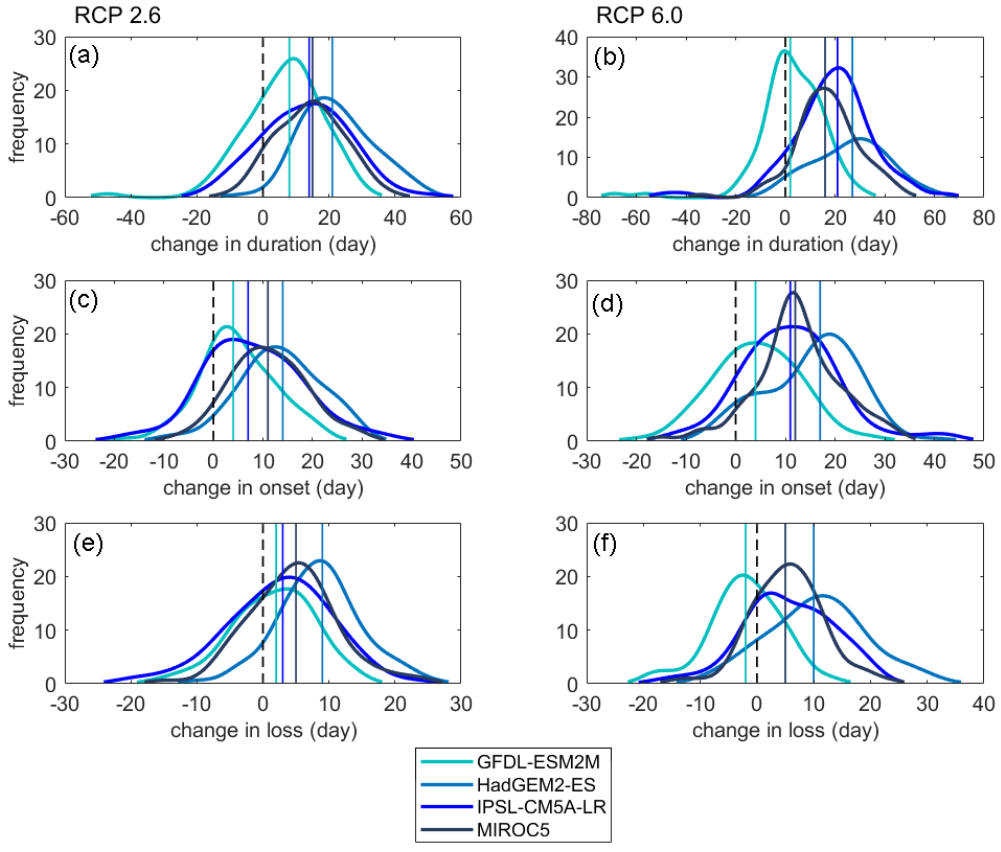

570 **Figure 6. Changes in the calculated annual anomalies of the (a)-(b) duration, (c)-(d) onset and (e)-(f) loss of stratification under (a)-(c)-(e) RCP 2.6 and (b)-(d)-(f) RCP 6.0, showing results from the lake model forced with daily GFDL-ESM2M, HadGEM2-ES, IPSL-CM5A-LR and MIROC5 projections. All changes are for 2006-2099 relative to 1975-2005. The median (vertical line) is also shown.**